Poly(*p*-phenyleneterephthalamide) and Poly(*m*-phenyleneisophthalamide): Positional Isomers with Partial Miscibility

S. M. Aharoni,* S. A. Curran, and N. S. Murthy

Allied-Signal Inc., Research and Technology, P.O. Box 1021, Morristown, New Jersey 07962-1021

Received March 9, 1992; Revised Manuscript Received April 28, 1992

ABSTRACT: The phase diagram of poly(*p*-phenyleneterephthalamide) (Pp-PT) and poly(*m*-phenyleneisophthalamide) (Pm-PI) was investigated by means of solid-state ^{13}C-NMR $T_{1\rho H}$ decay, WAXD, and DSC scans. It indicates only a limited range of polymer miscibility and wide compositional intervals in which several phases, amorphous and crystalline, coexist. The densities of the amorphous Pm-PI and the amorphous component of Pp-PT were measured and are sufficiently different to produce χ_{12} values and differences in solubility parameters large enough to explain the marginal solubility of the amorphous phases of Pp-PT and Pm-PI in each other.

Introduction

It is generally accepted that the cohesive energy, E_{coh}, of two chemically identical polymers is the same even when they are two positional isomers. The solubility parameter δ is defined as

$$\delta = (E_{coh}/V)^{1/2} \tag{1}$$

where V is the molar volume of a repeat unit. If the molar volumes of the chemically identical polymers 1 and 2 are identical, then

$$\delta_1 = \delta_2 \tag{2}$$

and the polymers are fully miscible. The Flory–Huggins lattice model leads to an estimation of the mutual miscibility of two *flexible nonpolar* polymers in terms of an interaction parameter χ_{12}:

$$\chi_{12} = (\delta_1 - \delta_2)^2 V/RT \tag{3}$$

where R is the gas constant and T is the absolute temperature. The definition of χ_{12} in terms of $(\delta_1 - \delta_2)^2$ leads to nonnegative χ_{12} values and does not allow a description of polymer pairs with strong attractive interactions where the polymers prefer to mix on a molecular scale and χ_{12} is negative. Furthermore, because it is couched in terms of the lattice model, the interaction parameter is not expected to describe the behavior of stiff and inflexible polymers.[2]

It has been theoretically shown by Flory[3] that a mixture of rodlike and random coil polymers thermodynamically prefers to segregate into two phases. If conditions are present to facilitate such phase separation, such as sufficient dilution, molecular mobility, and long enough time, then the phase separation will take place and the amount of the minority polymer in each growing phase will decrease with increasing chain length. These predictions were confirmed experimentally by Aharoni,[4,5] who concluded in a case of a ternary solution that "when either polymer is too flexible to form an anisotropic solution by itself, it will then separate from the ternary system into an isotropic phase, leaving the more rigid polymer in the coexisting anisotropic solution".[6] Linear, para-substituted aromatic polyamides such as poly(*p*-phenyleneterephthalamide) (Pp-PT) are stiff polymers, forming lyotropic liquid crystals in concentrated solution that are neither rodlike nor flexible. They may be called wormlike polymers. In the bulk they are partly crystalline with a measure of order and some parallel alignment of the stiff chains present also in the amorphous fraction. Therefore, it stands to reason that their amorphous component is more dense than the amorphous fraction of their flexible analogue, such as poly(*m*-phenyleneisophthalamide) (Pm-PI). If this is indeed the case, then the solubility parameter δ of Pp-PT should be different from that of Pm-PI, and if the difference is sufficiently large, the two chemically identical polymers will show a tendency toward phase separation. This tendency will depend not on the acutal formation of coexisting anisotropic and isotropic phases but on the dissimilar densities of two amorphous phases caused by the difference in the ability of wormlike and flexible chains to increase their levels of order by aligning themselves in parallel arrays. A gauge of the degree of order encountered in liquid crystalline systems can be obtained from the following experimental results.[7] Concentrated solutions (10.3–11.4%) of the polyamide poly(*p*-benzanilidyleneterephthalamide) (P-pBT) in concentrated H_2SO_4 were prepared at elevated temperatures. Upon cooling, the all underwent an isotropic to anisotropic transition. At that point, the order parameter $\langle P_2 \rangle$ was 0.4 in all cases. Upon further cooling, down to 50–70 K below the transition, the order parameter monotonically grew up to about 0.75–0.80. It never grew larger. We recall that in the bulk crystalline phase $\langle P_2 \rangle \sim 1.0$. The order parameter for a truly random flexible polymer is about zero. Hence, even in the absence of an anisotropic phase, a polymer that may form such a phase is capable of developing sufficient chain alignment for its order parameter to approach 0.4. The order parameter $\langle P_2 \rangle$ is defined as

$$\langle P_2 \rangle = [{}^1/_2(3\cos^2\beta - 1)] \tag{4}$$

where β is the angle describing the average tilt of the chain director relative to the macroscopic axis of sample orientation.

In this paper we investigate whether the two positionally isomeric aromatic polyamides Pp-PT and Pm-PI are compatible and whether their incompatibility may be attributed to a difference in amorphous density or to the tendency of Pp-PT to form liquid crystals.

Experimental Section

The investigated polymers were prepared from the diacids and diamines by the Yamazaki procedure[8] in *N,N*-dimethylacetamide (DMAc) containing 5 wt % dry LiCl. The polycon-

0024-9297/92/2225-4431$03.00/0

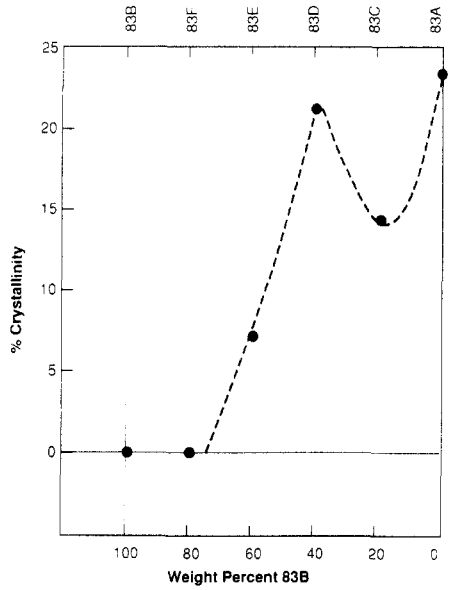

Figure 1. Percent crystallinity of aromatic polyamide blends of Pp-PT (83A) and Pm-PI (83B) as determined from WAXD scans.

densation was conducted at ca. 105 °C for 3 h and at a monomer concentration of ca. 7%. After completion, the reaction mixtures were poured into a large excess of methanol and filtered. The solid polymeric products were then successively washed in and filtered from tap water, boiling water, hot methanol, and methanol at ambient temperature to remove residual DMAc, LiCl, pyridine, triphenyl phosphite, diphenyl phosphite, phenol, and all other monomeric and short oligomeric reaction byproducts. The polymers were then dried to constant temperature under dynamic vacuum at 120 °C. For the polymerizations, all monomers, reagents, and solvents were obtained from Aldrich Chemical Co. at the highest available grade and were used without further purification.

Homogeneous blends were prepared by dissolving at room temperature the desired weights of Pp-PT and Pm-PI in concentrated H_2SO_4 to produce a single, dilute uniform and isotropic solution. The solution containing both polymers was then poured in a thin stream into an intensively stirred mixture of cold water and crushed ice. The rapidly coagulated polymer was pulverized in the cold mixture, and, after the ice melted, the polymer was filtered off and washed several times with water, then dilute sodium bicarbonate solution, and again water before drying in a vacuum oven at ca. 120 C. To ensure uniformity, the two parent polymers, Pp-PT and Pm-PI, were subjected to the same dissolution–precipitation process as their mixtures.

Dilute solution viscosities of concentrated H_2SO_4 solutions of the parent polymers were measured at 25 °C using Cannon-Ubbelohde internal dilution glass viscometers with solvent efflux times longer than 100 s. Densities of the solid Pp-PT and Pm-PI were measured at 21 °C in a glass pycnometer using mixtures of trichlorotrifluoroethane and hexanes.

Thermal studies were conducted by using a Du Pont Model 9900 differential scanning calorimeter (DSC). The heating and cooling rates were 20 K/min, always under a nitrogen atmosphere. Wide-angle X-ray diffraction (WAXD) scans were obtained in the parafocus mode on a Philips APD3600 diffractometer using copper radiation and a diffracted beam monochromator. The scans were analyzed using a modified version of the program SHADOW.[9,10] Data at $2\theta < 35°$ were used in the crystallinity calculations.

All NMR spectra were acquired at 25 °C on a Chemagnetics CMX-300 solid-state NMR spectrometer. For the blends, proton 90° pulses were 5 μs. Cross-polarization (CP) contact times were 900 μs with 50-kHz ^1H and ^{13}C spin lock for the results reported here. The proton decoupler strength was 90 kHz. The 50-kHz carbon spin lock hold times after CP varied between 10 μs and 25 ms. Cycle times were set to 3 s to allow complete proton spin–lattice relaxation. All samples were placed directly in a zirconia rotor and inserted in the Chemagnetics double-air-bearing magic-angle-spinning (MAS) probe (pencil probe). Spinning speeds were 6–7 kHz. The magic angle was set within 0.1° prior to analysis with a reference KBr sample, using the ^{79}Br sideband procedure.[11] Proton spin–lattice relaxation in the rotating frame rates ($T_{1\rho H}$) was measured according to Pines et al.[12] When plotted in the same figure, different relaxations are indicated by solid and empty circles for the sole purpose of easy recognition.

Results

The two synthesized polymers, poly(*p*-phenyleneterephthalamide)

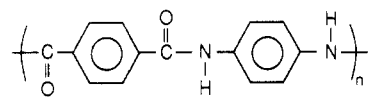

and poly(*m*-phenyleneisophthalamide)

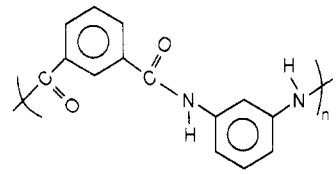

had intrinsic viscosities of 0.41 and 0.32 dL/g, respectively, corresponding[13,14] to number-average molecular weight, M_n, of about 2500 for both. Seeking the well-known advantage of higher compatibility of lower molecular weight (M) polymers, we elected to use these polymers instead of higher M homologues.

The WAXD patterns were all characterized by broad and relatively weak peaks. Even in the case of pure Pp-PT, the analyses indicate that a relatively small fraction of the material exists in a crystalline state. The breadths of the line widths, including the two crystalline ones at $2\theta \simeq 22.7°$ ($hkl = 200$) and $2\theta \simeq 43.2°$ ($hkl = 006$)[13] when present, indicate that the crystalline phase is either highly defective and/or the crystallites are very small. As can be seen in Figure 1, the crystalline fraction in the pure parent polymers Pp-PT and Pm-PI and in their blends never surpassed 25%, being zero for Pm-PI (83B) and its 80:20 blend with Pp-PT (coded 83F), rising to 7% in 60:40 Pm-PI/Pp-PT (83E), and the fluctuating from 21% to 14% to 23% upon changing from 40:60 Pm-PI/Pp-PT (83D) to 20:80 Pm-PI/Pp-PT (83C) to pure Pp-PT (83A), respectively.

The profile-fitted XRD scan of Pp-PT is shown in Figure 2a. The crystalline peaks in this scan are characteristic of the type II (modification II) crystal structure of Pp-PT identified by Haraguchi et al.[15] ($a = 7.94$ Å, $b = 5.12$ Å, $c = 12.9$ Å, monoclinic cell with $\gamma = 90°$ according to refs 15 and 16). Pp-PT crystallizes in the type II structure when allowed to coagulate in water from a sulfuric acid solution,[15] the method used in this study. Despite the differences in the positions of the crystalline peaks in the type I[17,18] and type II[15] structures, the diffuse scattering due to the amorphous component in both forms can be resolved into the same three components at 2θ values of 21, 27, and 42°. The 27 and 42° peaks correspond to the 002 and 004 reflections (c is the chain axis) and thus are due to the intrachain interference, i.e., the chain-axis structure. The 21° peak is due to the interchain interferences. The single peak is indicative of the pseudohexagonal packing of the relatively stiff polyamide chains. Since the amorphous domains can be considered as an assemblage of parallel cylinders over a range of at least 25 Å, the average interchain distance d_{av} can be calculated from the peak maximum using the relation $d_{av} =$

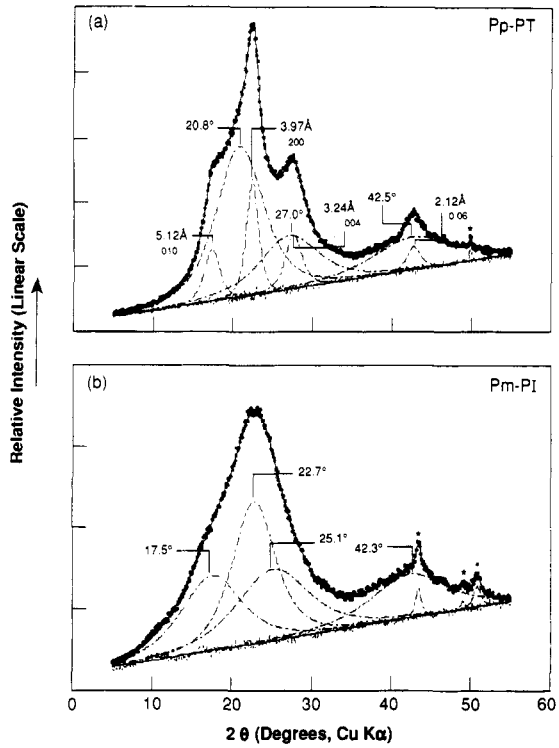

Figure 2. Profile-fitted XRD scans of Pp-PT (a) and Pm-PI (b) homopolymers. The observed intensities are shown with circles. The full line that overlaps the observed data represents the sum of the resolved components, which are shown as dashed lines. The dashed line over the base line (shown as a full line) is the difference between the observed intensities and the calculated curve. The amorphous peaks are identified by their 2θ values. The *hkl* indices of the crystalline peaks and the corresponding *d* spacings are shown for Pp-PT in (a). The sharp peaks marked with asterisks are probably due to impurities.

$1.11d_{Bragg}$.[19] The d_{av} for Pp-PT is 4.74 Å, and the average cross-sectional area per molecule calculated assuming a hexagonal lattice is 19.4 Å^2. Since the chains are far from being hexagonally close packed, the true cross-sectional area of Pp-PT in the amorphous phase would be greater than 19.4 Å^2. We will use this value *only* for comparing the cross-sectional area obtained under similar assumptions for Pm-PI.

The profile-fitted XRD scan of PM-PI is shown in Figure 2b. The polymer is mainly amorphous and the amorphous halo can be resolved into four distinct peaks at 17, 23, 25, and 42°. The chemical structures of Pm-PI and Pp-PT, and to some extent even their diffraction scans, are similar. Therefore, the amorphous peaks at 25 and 42° can be attributed to intrachain interference (chain-axis structure). Furthermore, the two halos at 17 and 23° are attributed to interchain interference in the equatorial plane. As with other liquid crystalline polyesters[20,21] and with flexible-chain polyesters,[22] these two equatorial amorphous peaks represent short-range ordering of the aromatic groups resulting from the alignment of these groups parallel to one another. In other words, rotational correlations of the adjacent aromatic group result in biaxial packing of the neighboring chains. This results in two interchain distance distributions, one in the plane of the aromatic groups (17° peak) and another normal to the plane (23° peak). The average distances corresponding to these two peaks can be calculated with the same assumptions used above for Pp-PT and are 5.6 and 4.3 Å, respectively. Assuming a 60° angle between these two directions, we obtain a cross-sectional area per molecule of 20.8 Å^2. This is 7% larger than the 19.4 Å^2 calculated for Pp-PT. This is not surprising since the Pm-PI chains are more flexible than the Pp-PT chains.

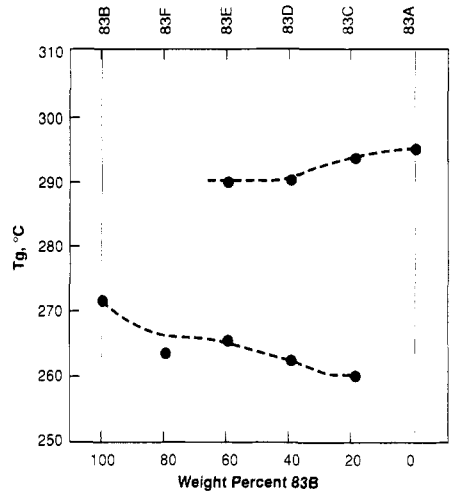

Figure 3. T_g of aromatic polyamides Pp-PT and Pm-PI and their blends (all coagulated in ice water from sulfuric acid solutions).

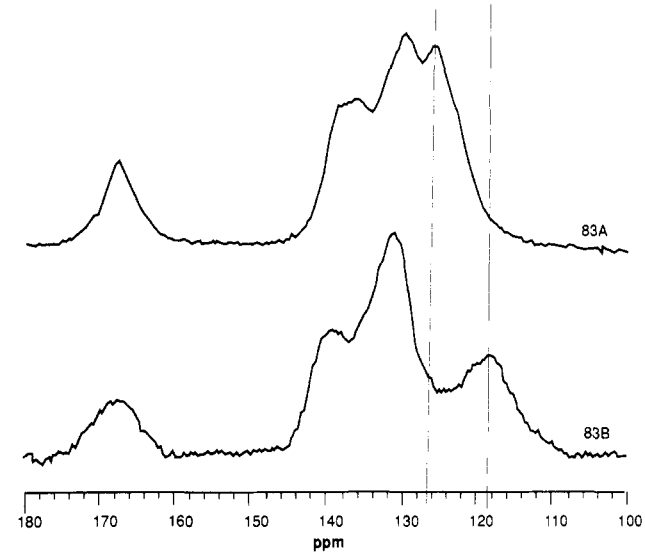

Figure 4. Solid-state carbon-13 NMR scans of Pp-PT (83A) and Pm-PI (83B).

The DSC scans were qualitatively consistent with the X-ray results. In Figure 3 are plotted the observed glass transition temperatures (T_g's) of the pure polymers and their blends. The T_g of pure Pm-PI (83B) is at ca. 272 °C and that of pure Pp-PT (83A) is at 295 °C. The 80:20 Pm-PI/Pp-PT blend shows only one T_g at 264 °C. This blend showed no crystallinity by X-ray techniques. All other blends, which showed varying fractions of crystalline matter, show two T_g's each. In all cases, the T_g's appear at temperatures lower than the corresponding T_g of the pure component. It is of interest to note here that a transition at ca. 350–360 °C appeared in all our DSC scans for Pm-PI, Pp-PT, and their blends. A transition at 345 °C is claimed in the literature to be the T_g of Pp-PT.[1] In light of the fact that such a transition appears also in the scan of Pm-PI, such a claim should be reconsidered.

As can be seen from Figure 4, the chemical shifts of the solid-state ^{13}C-NMR resonances of the stiff Pp-PT and flexible Pm-PI are sufficiently different, allowing their measurement independently of each other in the same blend. The $T_{1\rho H}$ relaxations were measured by following the decay of the resonance at 119 ppm for Pm-PI and the resonance at 127 ppm for Pp-PT. Homogeneous samples produce a single-exponential $T_{1\rho H}$ decay, appearing as a straight line on the conventional semilogarithmic plots

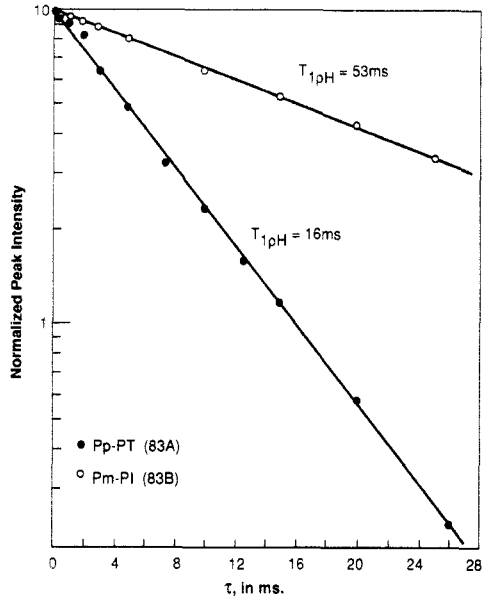

Figure 5. $T_{1\rho H}$ decay plots of Pp-PT (83A) and Pm-PI (83B). Solid and empty points are merely for the purpose of differentiating between different relaxations.

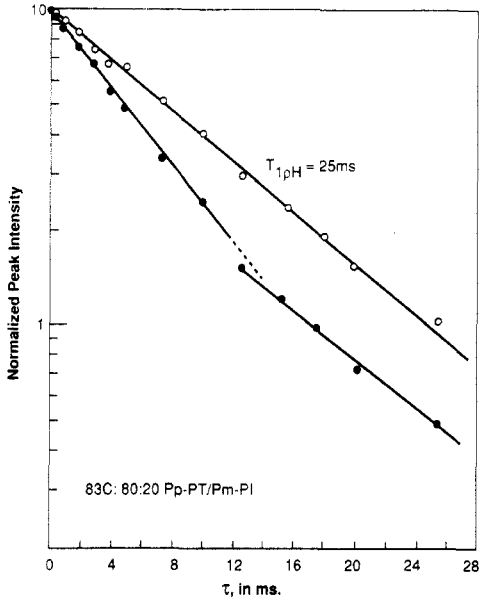

Figure 6. $T_{1\rho H}$ decay plot of blend 83C. See caption to Figure 5.

of peak intensity vs time. If the homogeneous phase contains more than one component, then the observed $T_{1\rho H}$ is a weighted average of the $T_{1\rho H}$'s of the individual components. If the sample is heterogeneous, then the decay curve will be curved or show a break in its slope. In Figure 5 are shown the decay curves of pure Pp-PT (83A) and pure Pm-PI (83B). Both show a single-exponential $T_{1\rho H}$ decay, and from the slopes of the curves we deduce that for Pp-PT, $T_{1\rho H}$ = 16 ms and for Pm-PI, $T_{1\rho H}$ = 53 ms. It is interesting that we do not detect a separate contribution of the crystalline phase in Pp-PT and in any of the blends containing this polymer.

The $T_{1\rho H}$ decay patterns of samples 83C (20:80 Pm-PI/Pp-PT) and 83F (80:20 Pm-PI/Pp-PT) in Figures 6 and 7, respectively, are similar in the respect that each contains a simple exponential decay, with $T_{1\rho H}$ = 25 ms for 83C and $T_{1\rho H}$ = 23.6 ms for 83F, and a multiple exponential decay appearing as a curvature in the decay. In these and subsequent figures, the empty circles describe Pm-PI response and the solid circles describe Pp-PT. The

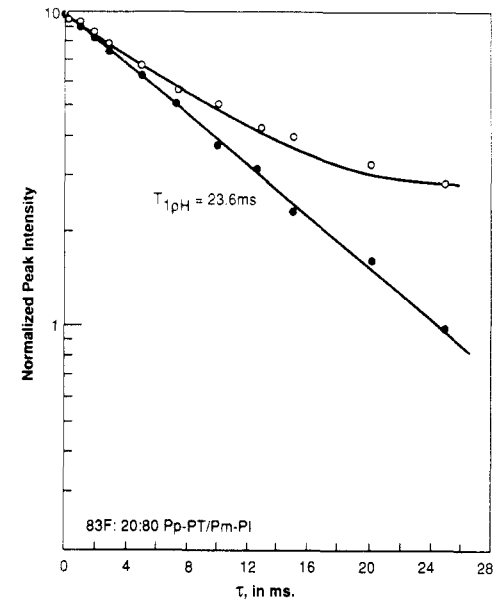

Figure 7. $T_{1\rho H}$ decay plot of blend 83F. See caption to Figure 5.

$T_{1\rho H}$ of 25–23.6 ms indicates the presence of ca. 25% Pm-PT and 75% Pp-PT in a single amorphous homogeneous phase. The curved lines in both Figures 6 and 7 indicate the coexistence in each sample of a nonhomogeneous phase together with the homogeneous phase described above. In sample 83C the inhomogeneous phase contains a majority of Pp-PT. Part of this inhomogeneous phase is characterized by a $T_{1\rho H}$ = 17 ms, very close to the $T_{1\rho H}$ = 16 ms of pure Pp-PT. In sample 83F, the multiexponential decay starts with $T_{1\rho H}$ = 23 ms, similar to the homogeneous 25:75 Pm-PI/Pp-PT, and gradually changes to $T_{1\rho H}$ = 68 ms, a decay rate slower than that for pure Pm-PI.

In the case of the 40:60 and 60:40 blends in samples 83D and 83E, respectively, two decay curves exist as in samples 83C and 83F, except that both curves of each sample show extensive curvature. In the case of 83D in Figure 8 (bottom), containing 40:60 Pm-PI/P-PT, the curvatures in both relaxation plots indicate a distribution of compositions on a nanometer scale, with no indication of a clear phase separation. Rather, there are Pm-PI-rich domains and Pp-PT-rich domains with a range of compositions between them. The relaxation of 83E in Figure 8 (top), containing 60:40 Pm-PI/Pp-PT, is more complex. One of the two curves can be fitted as the sum of two exponential decays, yielding $T_{1\rho H}$ = 16 ms for the initial slope and 24.7 ms for the later part of the curve. This is consistent with phase-separated pure Pp-PT and a mixture of 75:25 Pp-PT/Pm-PI. Assuming two overlapping exponentials, we calculate that in 83E, 30% of Pp-PT is completely phase separated and 70% is blended with Pm-PI. The second curve has an initial linear portion yielding $T_{1\rho H}$ = 25.2 ms, consistent with 75:25 Pp-PT/Pm-PI. The extensive curvature in the later stages of the relaxation makes it difficult to extract the quantity of phase-separated Pm-PI. If we assume, however, two overlapping exponentials where one $T_{1\rho H}$ is 24.7 ms and fit the data, then we may calculate 80% phase-separated Pm-PI and 20% Pm-PI blended with Pp-PT.

Density measurements by pycnometry yielded d = 1.4166 g/cm^3 for the Pp-PT sample 83A and d = 1.3234 g/cm^3 for the Pm-PI sample 83B. Previously measured density of 100% crystalline linear aromatic polyamides[13] gave an average density of 1.48 g/cm^3. In sample 83A, we measured close to 25% crystallinity. From these values,

Table I
Results of Solid-State ^{13}C-NMR $T_{1\rho H}$ Decay Studies

code	comp	phase state of Pm-PI component	phase state of Pp-PT component
83A	100% Pp-PT		single homogeneous phase
83B	100% Pm-PI	single homogeneous phase	
83C	80:20 83A/83B	in a homogeneous 3:1 83A/83B phase	ca. 70% in 3:1 83A/83B homogeneous phase + ca. 30% phase-separated 83A
83D	60:40 83A/83B	83B-rich heterogeneous phase	83A-rich heterogeneous phase
83E	40:60 83A/83B	ca. 20% in homogeneous 3:1 83A/83B phase + ca. 80% phase-separated 83B	ca. 70% in homogeneous 3:1 83A/83B phase + ca. 30% phase-separated 83A
83F	20:80 83A/83B	broad phase distribution: from ca. 5% in 3:1 83A/83B homogeneous phase, through a heterogeneous phase, to a small amount of phase-separated 83B	all 83A component in 3:1 83A/83B homogeneous phase

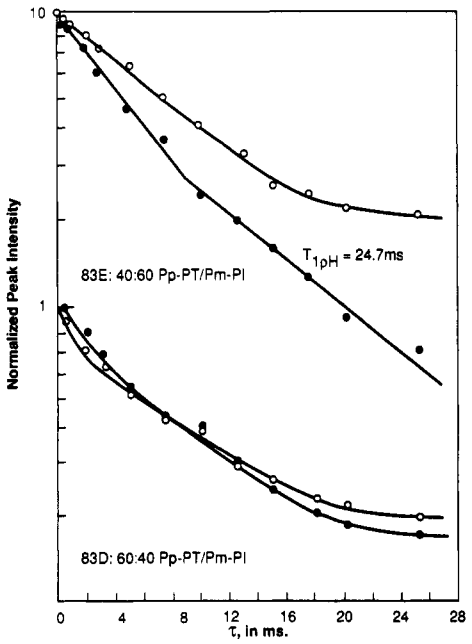

Figure 8. Top: $T_{1\rho H}$ decay plot of blend 83E. Bottom: $T_{1\rho H}$ decay plot of blend 83D. See caption to Figure 5.

we calculate the density of the amorphous fraction of 83A as [1.4166 − (0.25 × 1.48)]/0.75 = 1.395 g/cm^3. On the basis of experimental results, the density of the amorphous component in the Pp-PT sample 83A is 0.0716 g/cm^3 higher than the density of the fully amorphous Pm-PI sample 83B. If we use the density of 1.5 g/cm^3 calculated from crystallographic data[17,18] for the perfect Pp-PT crystal, we obtain a density of 1.39 g/cm^3 for the amorphous component in 83A, still 0.07 g/cm^3 denser than the fully amorphous 83B. This conclusion is in agreement with the XRD results discussed earlier.

Discussion

The results of the solid-state ^{13}C-NMR $T_{1\rho H}$ decay studies are listed in Table I. In the amorphous system, the repeated appearance of a homogeneous phase containing about a 3:1 ratio of Pp-PT to Pm-PI infers a stable phase with this composition. An excess of either polymer beyond this composition leads to the appearance of a second phase in the amorphous system. This amorphous phase appears to have a structure similar to that of Pm-PI as indicated in the XRD scans by the presence of a low-angle amorphous peak at $2\theta = 18°$ even at 80:20 composition (83C). The new phase may be a "pure" phase-separated Pp-PT as in the cases of 83C and 83E, or a "pure" phase-separated Pm-PI as in the cases of 83E and 83F. The heterogeneous phases observed in samples 83D and 83F are caused, we believe, by the rapid immobilization of the polymeric chains during the coagulation/precipitation step, arresting the process of phase separation before it could be completed and resulting in a spinodal decomposition. The difference between the mechanisms of spinodal decomposition and nucleation and growth is that in the former, the growing phases are not pure materials but each contains a gradation of compositions. The nucleation and growth mechanism involves the emergence of two pure phases.[23] The $T_{1\rho H}$ decays of the heterogeneous phases in this study indicate a gradation of composition on a nanometer scale, supporting our conviction that the heterogeneous phases detected in these studies are a manifestation of a spinodal decomposition mechanism of the phase separation of Pm-PI and the amorphous fraction of Pp-PT. This point, however, needs to be proven by further experiments.

When the results in Table I are evaluated, we should recall that a separate crystalline phase of the Pp-PT was not detected in the NMR experiments. This may be due to either or both of the following: (a) the chemical shifts of the amorphous and crystalline resonances of Pp-PT are indistinguishable from one another under the experimental conditions; (b) the $T_{1\rho H}$ relaxation rates of crystalline and amorphous phases may be equal. This is reasonable since our Pp-PT samples crystallize in the type II structure of Haraguchi et al.,[15] and this structure is less stable than the type I structure reported by Northolt et al.[17,18] Hence, the conformation of the Pp-PT chains in the crystalline regions could be similar to that in the amorphous domains. Additionally, XRD scans show that the crystalline phase of Pp-PT is very disordered, possibly due to a large number of crystal defects or very small crystallites or both. Thus, the chemical shifts and the $T_{1\rho H}$ relaxation rates of the crystalline domains could be indistinguishable from those of the amorphous domains. On the other hand, it may be that our NMR experiments fail to differentiate between the highly disorderd crystalline phase and the substantially ordered amorphous phase of Pp-PT; this order is reflected in the significantly higher density of the amorphous phase of Pp-PT as compared with Pm-PI. In this context, it is interesting to note, however, that the NMR technique appears to be more sensitive than either the DSC or the WAXD scans to detect the presence of finely dispersed phases in a complex system. This ability is especially evident in the case of sample 83F, where NMR detected three coexisting phases while DSC and WAXD showed only one.

Using eq 1, the densities measured above, and data in Van Krevelen's book,[1] we calculate the solubility parameter of Pm-PI as $\delta_{Pm-PI} = 30.91$ (mPa)$^{1/2}$, the solubility parameter of Pp-PT containing the crystalline fraction as $\delta_{Pp-PT} = 31.98$ (mPa)$^{1/2}$, and the solubility parameter of the amorphous component of Pp-PT as $\delta_{Pp-PT-a} = 31.73$ (mPa)$^{1/2}$ when the density of the amorphous phase is taken as 1.395 g/cm^3 and $\delta_{Pp-PT-a} = 31.55$ (mPa)$^{1/2}$ when the density of the amorphous part of Pp-PT is taken as 1.3788

g/cm^3. The largest $\delta_{Pp-PT} - \delta_{Pm-PI}$ is 31.98 − 30.91 = 1.07 (mPa)$^{1/2}$ and the smallest is 0.64 (mPa)$^{1/2}$. Using eq 3 we calculate the room temperature (21 °C) interaction parameters for the two extreme cases and obtain χ_{12} = 0.03934 and χ_{12} = 0.01446, respectively. Both the solubility parameter and interaction parameter differences between Pm-PI and the amorphous component of Pp-PT indicate that, on the basis of the difference in density alone, the two amorphous phases are expected to be only marginally compatible. This is indeed what was found by us experimentally. The differences in δ and χ_{12} are sufficiently large, and are expected to be much larger if the crystalline fraction of Pp-PT is compared with Pm-PI, that the arguments supporting the separation of rodlike from flexible-chain molecules[3] need not be invoked in the present case.

One final point: The solubility parameters in this study were calculated from group additivity and experimentally determined densities. They fell in the range $30.91 \leq \delta \leq 31.98$ (mPa)$^{1/2}$. These values are very close to the values of $31.2 \leq \delta \leq 32.8$ (mPa)$^{1/2}$ calculated recently by Rutledge and Suter[24] for various crystalline structures of Pp-PT. They are slightly higher than δ = 29 (mPa)$^{1/2}$ calculated for Pp-PT by Iyengar.[25] Both these calculations take into account the large intermolecular interactions present in Pp-PT. When such interactions are eliminated or minimized, as in the case of gels of isotropic rigid networks comprising stiff polyamide segments recently reported by Aharoni,[26] then the solubility parameter was demonstrated experimentally to be δ = 23.0 (mPa)$^{1/2}$. It is interesting to note that the relative contribution of the intermolecular interactions to the tensile modulus (E_3) and stiffness coefficient (C_{3333}) as reported by Rutledge and Suter[27] is about the same as the relative contribution of the intermolecular interactions to the solubility parameter.

Acknowledgment. It is our pleasure to acknowledge the help of M. F. Martin and C. Bednarczyk with several aspects of the experimental work.

References and Notes

(1) Van Krevelen, D. W. *Properties of Polymers*; Elsevier: Amsterdam, 1990; pp 189–225, 804–807.
(2) Coleman, M. M.; Graf, J. F.; Painter, P. C. *Specific Interactions and the Miscibility of Polymer Blends*; Technomic: Lancaster, PA, 1991; pp 340–343.
(3) Flory, P. J. *Macromolecules* **1978**, *11*, 1138.
(4) Aharoni, S. M. *Polymer* **1980**, *21*, 21.
(5) Aharoni, S. M. *Ferroelectrics* **1980**, *30*, 227.
(6) Aharoni, S. M. *J. Appl. Polym. Sci.* **1980**, *25*, 2891.
(7) Picken, S. J. *Macromolecules* **1990**, *23*, 464.
(8) Yamazaki, N.; Matsumoto, M.; Higashi, F. *J. Polym. Sci., Polym. Chem. Ed.* **1975**, *13*, 1373.
(9) Howard, S. A. *Adv. X-ray Anal.* **1989**, *32*, 523.
(10) Murthy, N. S.; Minor, H. *Polymer* **1990**, *31*, 996.
(11) Frye, J. S.; Maciel, G. E. *J. Magn. Reson.* **1982**, *48*, 125.
(12) Pines, A.; Gibby, M.; Waugh, J. S. *J. Chem. Phys.* **1973**, *59*, 569.
(13) Aharoni, S. M. *Macromolecules* **1987**, *20*, 2010.
(14) Aharoni, S. M. *Macromolecules* **1988**, *21*, 185.
(15) Haraguchi, K.; Kajiyama, T.; Takayanagi, M. *J. Appl. Polym. Sci.* **1979**, *23*, 903, 915.
(16) Rutledge, G. C.; Suter, U. W.; Papaspyrides, C. D. *Macromolecules* **1991**, *24*, 1934.
(17) Northolt, M. G.; Van Aartsen, J. J. *J. Polym. Sci., Polym. Lett. Ed.* **1973**, *11*, 333.
(18) Northolt, M. G. *Eur. Polym.* **1974**, *10*, 799.
(19) Klug, H. P.; Alexander, L. E. *X-ray Diffraction Procedures*; Wiley: New York, 1974; p 849.
(20) Thomas, E. L.; Wood, B. A. *Faraday Discuss. Chem. Soc.* **1985**, *79*, 229.
(21) Mitchell, G. R.; Windle, A. H. *Polymer* **1982**, *23*, 1269.
(22) Murthy, N. S.; Correale, S. T.; Minor, H. *Macromolecules* **1991**, *24*, 1185.
(23) Olabisi, O.; Robeson, L. M.; Shaw, M. T. *Polymer–Polymer Miscibility*; Academic Press: New York, 1979; pp 19–116.
(24) Rutledge, G. C.; Suter, U. W. *Macromolecules* **1991**, *24*, 1921.
(25) Iyengar, Y. *J. Appl. Polym. Sci.* **1978**, *22*, 801.
(26) Aharoni, S. M. *J. Appl. Polym. Sci.* **1992**, *45*, 813.
(27) Rutledge, G. C.; Suter, U. W. *Polymer* **1991**, *32*, 2179.

Registry No. Pp–PT (copolymer), 25035-37-4; Pp–PT (SRU), 24938-64-5; Pm–PI (copolymer), 25035-33-0; Pm–PI (SRU), 24938-60-1.